20

Possibilities of Deriving Crop Evapotranspiration from Satellite Data with the Integration with Other Sources of Information

Gheorghe Stancalie and Argentina Nertan
National Meteorological Administration 97,
Soseaua Bucuresti-Ploiesti, Bucharest
Romania

1. Introduction

After precipitation, evapotranspiration is one of the most significant components in terrestrial water budgets.

Evapotranspiration (ET) describes the transport of water into the atmosphere from surfaces (including soil - soil evaporation) and from vegetation (transpiration). Those are often the most important contributors to evapotranspiration. Other contributors to evapotranspiration are the e from wet canopy surface (wet-canopy evaporation) and evaporation from vegetation-covered water surface in wetlands the process of evapotranspiration is one of the main consumers of solar energy at the Earth's surface. The energy used for evapotranspiration is generally referred to as latent heat flux. The term latent heat flux includes other related processes unrelated to transpiration including condensation (e.g., fog, dew), and snow and ice sublimation.

There are several factors that affect the evapotranspiration processes: energy availability; the humidity gradient away from the surface(the rate and quantity of water vapor entering into the atmosphere are higher in drier air); the wind speed at the soil level (wind affects evapotranspiration by bringing heat energy into an area); Water availability (it is well known that the evapotranspiration cannot occur if water is not available); Vegetation biophysical parameters (many physical parameters of the vegetation, like cover plant height, leaf area index and leaf shape and the reflectivity of plant surfaces can affect evapotranspiration); Stomatal resistance (the transpiration rate is dependent on the diffusion resistance provided by the stomatal pores, and also on the humidity gradient between the leaf's internal air spaces and the outside air); soil characteristics which includes its heat capacity, and soil chemistry and albedo. For a given climatic region the evapotranspiration follows the seasonal declination of solar radiation and the resulting air temperatures: minimum evapotranspiration rates generally occur during the coldest months of the year and maximum rates generally coincide with the summer season (Burba, 2010). Even so evapotranspiration depends on solar energy; the availability of soil moisture and plant maturity, the seasonal maximum evapotranspiration actually may precede or follow the

seasonal maximum solar radiation and air temperature by several weeks (Burba, 2010). If the moisture is available, evapotranspiration is dependent mainly on the availability of solar energy to vaporize water: evapotranspiration varies with latitude, season, time of day, and cloud cover. Most of the evapotranspiration of water at the Earth's surface level occurs in the subtropical regions (Fig.1). In these areas, high quantities of solar radiation provide the energy necessary to convert liquid water into a gas. Usually, evapotranspiration exceeds precipitation on middle and high latitude large areas during the summer season. As a result of climate change it is expected to induce a further intensification of the global water cycle, including ET (Huntington, 2006). Therefore accurate estimates of evapotranspiration are needed for weather forecasting and projecting the long-term effects of land use change and global climate change, irrigation scheduling and watershed management.

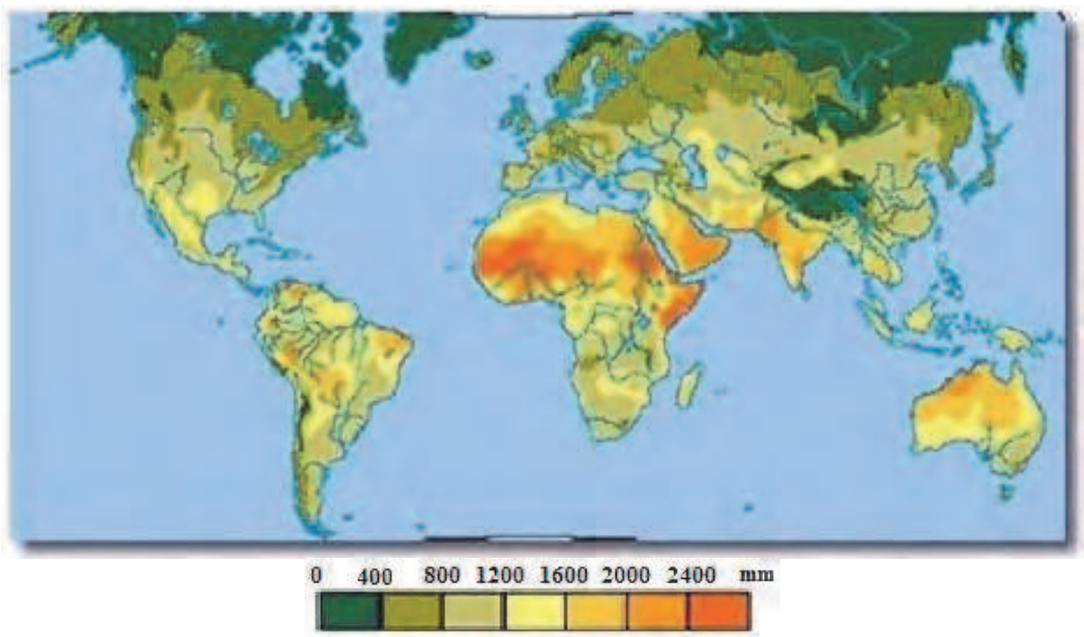

Fig. 1. Mean Annual Potential Evapotranspiration (UNEP World Atlas of Desertification)

In this regard, remote sensing data with the increasing imagery resolution is a useful tool to provide ET information over different temporal and spatial scales. During the last decades important progresses were made in the determination of ET using remote sensing techniques. Some studies have classified the methods of ET estimation in two categories: semi- empirical methods - use empirical relationship and a minimum set of meteorological data; analytical methods – consist in the establishment of the physical process at the scale of interest. A study done by Courault (2007) proposed a few methods which can be classified as follows: empirical direct methods, residual methods of the energy budget, deterministic methods, and vegetation index methods.

In agriculture, an accurate quantification of ET is important for effective and efficient irrigation management. When evaporative demand exceeds precipitation, plant growth and quality may be unfavorably affected by soil water deficit. A large part of the irrigation water applied to agricultural lands *(Fig. 2)* is consumed by evaporation and transpiration. In a given crop, evapotranspiration process is influenced by several factors: plant species,

canopy characteristics, plant population, degree of surface cover, plant growth stage, irrigation regime (over irrigation can increase ET due to larger evaporation), soil water availability, planting date, tillage practice, etc. As it can be observed from Fig. 2 the movement of the water vapor from the soil and plant surface, a t a field level is influenced mainly by wind speed and direction although other climatic factors also can play a role. Evapotranspiration increases with increasing air temperature and solar radiation. Wind speed can cause ET increasing. For high wind speed values the plant leaf stomata (the small pores on the top and bottom leaf surfaces that regulate transpiration) close and evapotranspiration is reduced. There are situations when wind can cause mechanical damage to plants which can decrease ET due to reduced leaf area. Hail can reduce also leaf area and evapotranspiration. Higher relative humidity decreases ET as the demand for water vapor by the atmosphere surrounding the leaf surface decreases. If relative humidity (dry air) has lower values, the ET increases due to the low humidity which increases the vapor pressure deficit between the vegetation surface and air. On rainy days, incoming solar radiation decreases, relative humidity increases, and air temperature usually decreases, generation ET decreasing. But, depending on climatic conditions, actual crop water use usually increases in the days after a rain event due to increased availability of water in the soil surface and crop root zone.

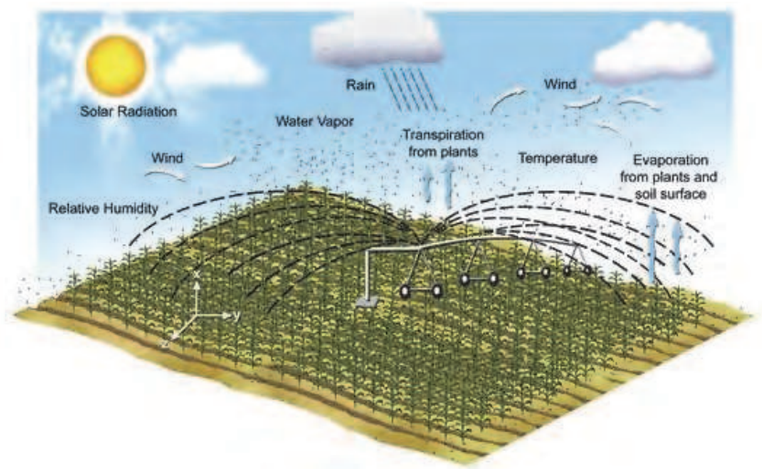

Fig. 2. Evaporation and transpiration and the factors that impact these processes in an irrigated crop.

2. Evapotranspiration and energy budget

The estimation of ET parameter, corresponding to the latent heat flux (λE) from remote sensing is based on the energy balance evaluation through several surface properties such as albedo, surface temperature (T_s), vegetation cover, and leaf area index (LAI). Surface energy balance (SEB) models are based on the surface energy budget equation. To estimate regional crop ET, three basic types of remote sensing approaches have been successfully applied (Su, 2002).

The first approach computes a surface energy balance (SEB) using the radiometric surface temperature for estimating the sensible heat flux (H), and obtaining ET as a residual of the

energy balance. The single-layer SEB models implicitly treat the energy exchanges between soil, vegetation and the atmosphere and compute latent heat flux (λE) by evaluating net (all-wave) radiant energy (R_n), soil heat flux (G) and H. For instantaneous conditions, the energy balance equation is the following:

$$\lambda E = R_n - H - G \quad (1)$$

where: R_n = net radiant energy (all-wave); G = soil heat flux; H = sensible heat flux (Wm^{-2}); λE = latent energy exchanges (E = the rate of evaporation of water (kg m^{-2} s^{-1}) and λ = the latent heat of vaporization of water (J kg^{-1})). λE is obtained as the residual of the energy balance contain biases from both H and (R_n - G). There are several factors which affect the performance of single-source approaches, like the uncertainties about atmospheric and emissivity effects. LST impacts on all terms of the energy balance in particular on long wave radiation. The radiative surface temperatures provided by an infrared radiometer from a space borne platform are measured by satellite sensors such as LANDSAT, AVHRR, MODIS and ASTER. Converting radiometric temperatures to kinetic temperature requires considerations about surface emissivity (λE), preferably from ground measurements. Remotely LST is subject to atmospheric effects which are primarily associated with the absorption of infrared radiation by atmospheric water vapor and which lead to errors of 3–5 K. A wide range of techniques have been developed to correct for atmospheric effects, including: single-channel methods; split-window techniques; multi-angle methods and combinations of split-window and multi-channel methods. Radiant and convective fluxes can be described: by considering the observed surface as a single component (single layer approaches); by separating soil and vegetation components with different degrees of canopy description in concordance with the number of vegetation layers (multilayer approaches). Net radiant energy depends on the incident solar radiation (R_g), incident atmospheric radiation over the thermal spectral domain (R_a), surface albedo (α_s), surface emissivity (ε_s) and surface temperature (T_s), according to the following equation:

$$R_n = (1 - \alpha_s)R_g + \varepsilon_s R_a - \varepsilon_s \sigma T_s^4 \quad (2)$$

For single layer models, R_n is related to the whole surface and in the case of multiple layer models, R_n is linked with both soil and vegetation layers. For single approaches, sensible heat flux H is estimated using the aerodynamic resistance between the surface and the reference height in the lower atmosphere (usually 2 m) above the surface. Aerodynamic resistance (r_a) is a function of wind speed, atmospheric stability and roughness lengths for momentum and heat. For multiple layer models, H is characterized taking into account the soil and canopy resistance, with the corresponding temperature:

$$H = \rho c_p \frac{(T_s - T_a)}{r_a} \quad (3)$$

Eq. (3) shows that the estimation of λE parameter can be made using the residual method, which induces that λE is linearly related to the difference between the surface temperature (T_s) and air temperature (T_a) at the time of T_s measurement if the second order dependence of r_a on this gradient is ignored.

$$\lambda E = R_n - G - \rho cp \frac{(T_s - T_a)}{r_a} \quad (4)$$

Equation (4) is usually used to estimate λE. At midday, it provides a good indicator regarding the plant water status for irrigation scheduling. For λE estimation over longer periods (daily, monthly, seasonal estimations), the use of ground-based ET from weather data is necessary to make temporal interpolation. Some studies have used the trend for the evaporative fraction (EF), such as the ratio of latent heat flux to available energy for convective fluxes, to be almost constant during the daytime. This allows estimating the daytime evaporation from one or two estimates only of EF at midday, for example at the satellite acquisition time (Courault et al., 2005).

$$EF = \frac{\lambda E}{R_n - G}, \quad ET_{24} = EF * R_{n24} \tag{5}$$

ET can be estimated from air vapor pressure (p_a) and a water vapor exchange coefficient (h_s) according to the following equation:

$$\lambda E = \rho c_p h_s (p_s^*(T_s) - e_a) \tag{6}$$

Usually this method is used in models simulating Soil–Vegetation–Atmosphere Transfers (SVAT). $p_s^*(T_s)$ represent the saturated vapor pressure at the surface temperature T_s and h_s is the exchange coefficient which depends on the aerodynamic exchange coefficient ($1/r_a$), soil surface and stomatal resistances of the different leaves in the canopy. Katerji & Perrier (1985) estimated a global canopy resistance (r_g) including both soil and canopy resistances (equation 6)

$$r_g = \frac{1}{\frac{1}{r_{veg} + r_w} + \frac{1}{r_0 + r_s}} \tag{7}$$

where: r_{veg} is the resistance due to the vegetation structure, r_w the resistance of the soil layer depending on the soil water content, r_0 the resistance due to the canopy structure and r_s the bulk stomatal resistance. To calculate this parameters it necessary to have information regarding the plant structure like LAI and fraction of vegetation cover (FC), the minimum stomatal resistance (r_{smin}). Many studies proposed various parameterizations of the stomatal resistance taking into account climatic conditions and soil moisture (Jacquemin & Noilhan, 1990). This proves that the ($T_s - T_a$) is related to ET term, and that Ts can be estimated using thermal infrared measurements (at regional or global scale using satellite data, and at local scale using ground measurements).

The second approach uses vegetation indices (VI) derived from canopy reflectance data to estimate basal crop coefficient (K_{cb}) that can be used to convert reference ET to actual crop ET, and requires local meteorological and soil data to maintain a water balance in the root zone of the crop. The VIs is related to land cover, crop density, biomass and other vegetation characteristics. VIs such as the Normalized Difference Vegetation Index (NDVI), the Soil Adjusted Vegetation Index (SAVI), the Enhanced Vegetation Index (EVI) and the Simple Ratio (SR), are measures of canopy greenness which may be related to physiological processes such as transpiration and photosynthesis. Among the relatively new satellite sensors it has to be mentioned the advantages of using MODIS/Aqua that offer improved spectral and radiometric resolution for deriving surface temperatures and vegetation indices, as well as increased frequency of evaporative fraction and evaporation estimates when compared with other sensors. The observed spatial variability in radiometric surface

temperature is used with reflectance and/or vegetation index observations for evaporation estimation. For ET estimation from agricultural crops the most direct application is to substitute the VIs for crop coefficients (defined as the ratio between actual crop water use and reference crop evaporation for the given set of local meteorological conditions). Negative observing correlations between the NDVI and radiometric surface temperature could be linked to evaporative cooling, although for most landscapes variations in fractional vegetation cover, soil moisture availability and meteorological conditions will cause considerable scatter in those relationships. The methods associated with this approach generate spatially distributed values of K_{cb} that capture field-specific crop development and are used to adjust a reference ET (ET_o) estimated daily from local weather station data.

The third approach uses remotely sensed LST with Land Surface Models (LSMs) and Soil–Vegetation–Atmosphere (SVAT) models, developed to estimate heat and mass transfer at the land surface. LSMs contain physical descriptions of the transfer in the soil–vegetation–atmosphere continuum, and with proper initial and boundary conditions provide continuous simulations when driven by weather and radiation data. The energy-based LSMs are of particular interest because these approaches allow for a strong link to remote sensing applications. The use of the spatially distributed nature of remote sensing data as a calibration source has been limited, with the focus placed on data assimilation approaches to update model states, rather than inform the actual model structure. Data assimilation is the incorporation of observations into a numerical model(s) with the purpose of providing the model with the best estimate of the current state of a system. There are two types of data assimilation: (i) sequential assimilation which involves correcting state variables (e.g. temperature, soil moisture) in the model whenever remote sensing data are available; and (ii) variation assimilation when unknown model parameters are changed using data sets obtained over different time windows. Remotely sensed LSTs have been assimilated at point scales into various schemes for estimating land surface fluxes by comparing simulated and observed temperatures and adjusting a state variable (e.g. soil moisture) or model parameters in the land surface process model. Such use of remote sensing data has highlighted problems of using spatial remote sensing data with spatial resolutions of tens or hundreds of kilometers with point-scale SVAT models and has led to the search for ''effective'' land surface parameters. There exist no effective means of evaluating ET spatially distributed outputs of either remote sensing based approaches or LSMs at scales greater than a few kilometers, particularly over non-homogeneous surfaces. The inability to evaluate remote sensing based estimates in a distributed manner is a serious limitation in broader scale applications of such approaches. It must be noted here that ET evaluation of remote sensing based approaches with ground based data tends to favour those few clear sky days when fluxes are reproduced most agreeably, and on relatively flat locations.

In this case the radiation budget is given by the following equation (Kalma et al., 2008):

$$R_n = K\downarrow - K\uparrow + L\downarrow - L\uparrow \tag{8}$$

where K↓ is the down-welling shortwave radiation and it depends on atmospheric transmissivity, time of the day, day of the year and geographic coordination. K↑ represents the reflected shortwave radiation which depends on K↓ and surface albedo (a), L↓ is the down-welling long wave radiation and L↑ is the up-welling long wave radiation. L↓ depends on the atmospheric emissivity (which in turn is influenced by amounts of atmospheric water vapor, carbon dioxide and oxygen) and by air temperature. L↑ si influenced by land surface temperature and emissivity

3. Direct methods using difference between surface and air temperature

Mapping daily evapotranspiration over large areas considering the surface temperature measurements has been made using a simplified relationship which assumes that it is possible to directly relate the daily (λE_d) to the difference $(T_{rad} - T_a)_i$ between (near) mid-day observations (i) of surface temperature and near-surface air temperature (Ta) measured at midday as follows:

$$\lambda E_d = (R_n)_d - B(T_{rad} - T_a)_i^n \quad (9)$$

B is a statistical regression coefficient which depends on surface roughness. n depends on atmospheric stability. Equation 9 was derived from Heat Capacity Mapping Mission (HCMM) observations over fairly homogeneous irrigated and non-irrigated land surfaces, with areas between 50 and 200 km^2 (Seguin et al. 1982a, b). Some authors as Carlson et al. (1995a) proposed a simplified method based on Eq. 9 which uses the difference ($T_{rad} - T_a$) at 50 m at the time of the satellite overpass. They showed that B coefficient and n are closely related to fractional cover f_c that can be obtained from the NDVI–T_{rad} plots. B values vary from 0.015 for bare soil to 0.065 for complete vegetation cover and n decreased from 1.0 for bare soil to 0.65 for full cover.

4. Surface energy balance models

Surface energy balance models (SEBAL) assume that the rate of exchange of a quantity (heat or mass) between two points is driven by a difference in potential (temperature or concentration) and controlled by a set of resistances which depend on the local atmospheric environment and the land surface and vegetation properties. In the review made by Overgaard et al. (2006) regarding the evolution of land surface energy balance models are described the following approaches: the combination approach by Penman (1948) which developed an equation to predict the rate of ET from open water, wet soil and well-watered grass based on easily measured meteorological variables such as radiation, air temperature, humidity, and wind speed; the Penman–Monteith ''one-layer'', ''one-source'' or ''big leaf'' models (Monteith 1965) which recognize the role of surface controls but do not distinguish between soil evaporation and transpiration; this approach estimates ET rate as a function of canopy and boundary layer resistances; ''two-layer'' or ''two-source'' model such as described by Shuttleworth and Wallace (1985) which includes a canopy layer in which heat and mass fluxes from the soil and from the vegetation are allowed to interact; multi-layer models which are essentially extensions of the two-layer approach.

4.1 The Penman–Monteith, ''one-source'' SEB models

The Penman–Monteith (PM) approach combines energy balance and mass transfer concepts (Penman, 1948) with stomatal and surface resistance (Monteith, 1981). Most "one source" SEB models compute λE by evaluating R_n, G and H and solve for λE as the residual term in the energy balance equation (see Eq. 10). The sensible heat flux (H) is given by:

$$H = \rho C_p \left[\frac{(T_{ad} - T_a)}{r_a}\right] \quad (10)$$

Where: ρ = air density (kg*m^{-3}); C_p = specific heat of air at constant pressure (J kg^{-1} K^{-1}); T_{ad} = aerodynamic surface temperature at canopy source height (K); T_a = near surface air

temperature (K); r_a = aerodynamic resistance to sensible heat transfer between the canopy source height and the bulk air at a reference height above the canopy (s m^{-1}). The r_a term is usually calculated from local data on wind speed, surface roughness length and atmospheric stability conditions. According to Norman and Becker (1995), the aerodynamic surface temperature (T_{ad}) represent the temperature that along with the air temperature and a resistance calculated from the log-profile theory provides an estimate H. The key issue of PM approach is to estimate an accurately sensible heat flux. T_{ad} is obtained by extrapolating the logarithmic air temperature profile to the roughness length for heat transport (z_{oh}) or, more precisely, to (d + z_{oh}) where d = zero-plane displacement height. Usually, due to the fact that T_{ad} cannot be measured using remote sensing, it is replaced with T_{rad}. As it is demonstrated by Troufleau et al. (1997), for dense canopy T_{rad} and T_{ad} may differ with 1-2 K and much more for sparse canopy. Surface temperature ($T_{rad)}$ is related to the kinetic temperature by the surface emissivity (ε) (Eq, 11) and it depends on view angle (θ) (Norman et. al, 2000). On the other hand T_{ad} and aerodynamic resistance are fairly difficult to obtain for non-homogenous land surfaces.

$$T_{rad} = \varepsilon^{1/4} * T_k \tag{11}$$

The aerodynamic resistance r_a can be calculated with the following equation:

$$r_a = \frac{1}{k^2} u \left[ln \frac{z-d}{z_{oh}} - \Psi_h \frac{z-d}{L} \right] \left[ln \frac{z-d}{z_{om}} - \Psi_m \frac{z-d}{L} \right] \tag{12}$$

where: k = 0.4 (von Karman's constant); u = wind speed at reference height z (m s^{-1}); d = zero-plane displacement height (m); z_{oh} and z_{om} = roughness lengths (m) for sensible heat and momentum flux, respectively; Ψ_h and Ψ_m = stability correction functions for sensible heat and momentum flux, respectively; L = Monin-Obukhov length L (m). The $\Psi_h = 0$ and $\Psi_m = 0$ if near surface atmospheric conditions are neutrally stable. Usually, the aerodynamic resistance is estimated from local data, even that area averaging of roughness lengths is highly non-linear (Boegh et al. 2002). Several studies, such as Cleugh at al. (2007) used these equations for evapotranspiration landscape monitoring. Their approach estimates E at 16-day intervals using 8-day composites of 1 km MODIS T_{rad} observations and was tested with 3 years of flux tower measurements and was obtained significant discrepancies between observed and simulated land surface fluxes, generated by the following factors: the estimation of H with Eqs. 9 and 10 is not constrained by the requirement for energy conservation; errors in z_{oh} determination; use of unrepresentative emissivities; using time-averages of instantaneous T_{rad}, T_a and R_n, the non-linearity of Eq. 9 may cause significant errors; standard MODIS data processing eliminates all cloud-contaminated pixels in the composite period. Bastiaanssen et al. (1998a) developed a calibration procedure using image data to account for the differences between T_{aero} and T_{rad}, which are important, mainly for incomplete vegetation covers. Other authors, such as Stewart et al. (1994) and Kustas et al. (2003a), made empirical adjustments to aerodynamic resistance, related to z_{oh} (eq. 13).

$$H = \rho C_p \left[\frac{T_{rad}(\Theta) - T_a}{r_a - r_{ex}} \right] \tag{13}$$

where: T_{rad} (θ) =radiometric surface temperature (K) at view angle θ derived from the satellite brightness temperature; r_{ex} = excess resistance (s m^{-1}) (reflects differences between

momentum and sensible heat transfer. According to Stewart et al. (1994) r_{ex} is function of the ratio of roughness lengths for momentum z_{om} and for sensible heat z_{oh} and the friction velocity u* (m s^{-1}) (eq. 14):

$$r_{ex} = \frac{kB^{-1}}{ku^*} = ln\frac{z_{om}/z_{oh}}{ku^*} \quad (14)$$

where kB^{-1} = dimensionless ratio determined by local calibration. Eq. 14 assumes that the ratio z_{om}/z_{oh} may be treated as constant for uniform surfaces, although kB^{-1} has been found to be highly variable (Brutsaert 1999).

In the case of the one source Surface Energy Balance System (SEBS) (Su, 2002) the surface heat fluxes are estimated from satellite data and available meteorological data. There are three sets of input data in SEBS: the first set includes the following parameters: α, ε, T_{rad}, LAI, fractional vegetation coverage and the vegetation height (if the vegetation information is not explicitly available, SEBS can use as input data the Normalized Difference Vegetation Index (NDVI)); the second set includes T_a, u, actual vapour pressure (e_a) at a reference height as well as total air pressure; the third set of data consists of measured (or estimated) K↓ and L↓. For R_n, G, and the partitioning of (R_n - G) into H and λE, SEBS use different modules (Fig. 3): H is estimated using Monin–Obukhov similarity theory; in the case of u and vegetation parameters (height and LAI) is used the Massman (1997) model to to estimate the displacement height (d) and the roughness height for momentum (z_{om}); the equations proposed by Brutsaert (1982, 1999) are used when only the height of the vegetation is available. The SEBS was successfully tested for agricultural areas, grassland and forests, across various spatial scales. Several studies used flux tower method and data from Landsat, ASTER ad Modis sensors (Su et al. 2005, 2007, McCabe and Wood 2006).

The Fig. 4 shows the time series, determined during the Soil Moisture Atmosphere Coupling Experiment 2002 (SMACEX-02) (Kustas et al. 2005). These time series illustrates latent heat fluxes and sensible heat fluxes measured with in situ eddy-covariance equipment (closed) together with SEBS model (open) over a field site (corn) from Iowa. The gaps in the time series are caused either the missing ancillary data or absence of flux measurements. Many factors influence the single-source approach: there are uncertainties due to atmospheric and emissivity effects; because of the vegetation properties and of the angle view, the relationship between T_{ad} and T_a is not unique; this approach requires representative near-surface T_a and other meteorological data measured (or estimated) at the time of the satellite overpass at a location closely with the T_{rad} observation. This can generate errors in defining meteorological parameter for each satellite pixel from a sparse network of weather stations (at the time of satellite overpass), mainly for areas with high relative relief and slopes. Another important factor is that the accuracy of any of the estimates depends on the performance of the algorithm used for temperature retrieval.

The major advantages of SEBS are: uncertainty due to the surface temperature or meteorological variables can be limited taking into account the energy balance at the limiting cases; through the SEBS was formulated a new equation for the roughness height for heat transfer, using fixed values; a priori knowledge of the actual turbulent heat fluxes is not required. Another single-source energy balance models, developed based on the conception of SEBAL, are S-SEBI (Simplified-SEBI), METRIC (Mapping EvapoTranspiration at high Resolution with Internalized Calibration), etc. The main difference between such kinds of models is the difference in how they calculate the sensible heat, i.e. the way to define the dry (maximum sensible heat and minimum latent heat) and wet (maximum latent

heat and minimum sensible heat) limits and how to interpolate between the defined upper and lower limits to calculate the sensible heat flux for a given set of boundary layer parameters of remotely sensed data (T_s, albedo, NDVI, LAI) and ground-based air temperature, wind speed, humidity. The assumptions in all these models are that there are few or no changes in atmospheric conditions (especially the surface available energy) in space and sufficient surface horizontal variations are required to ensure dry and wet limits existed in the study area.

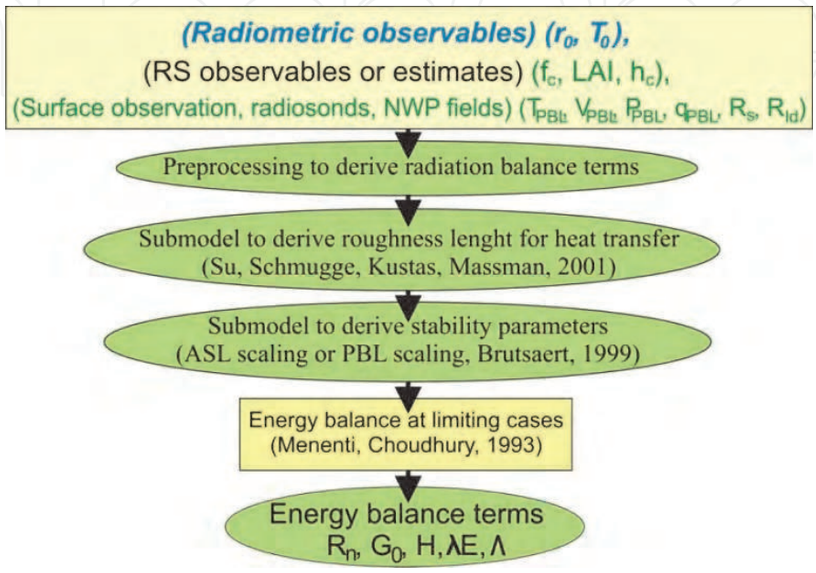

Fig. 3. Schematic representation of SEBS (after Su, 2008)

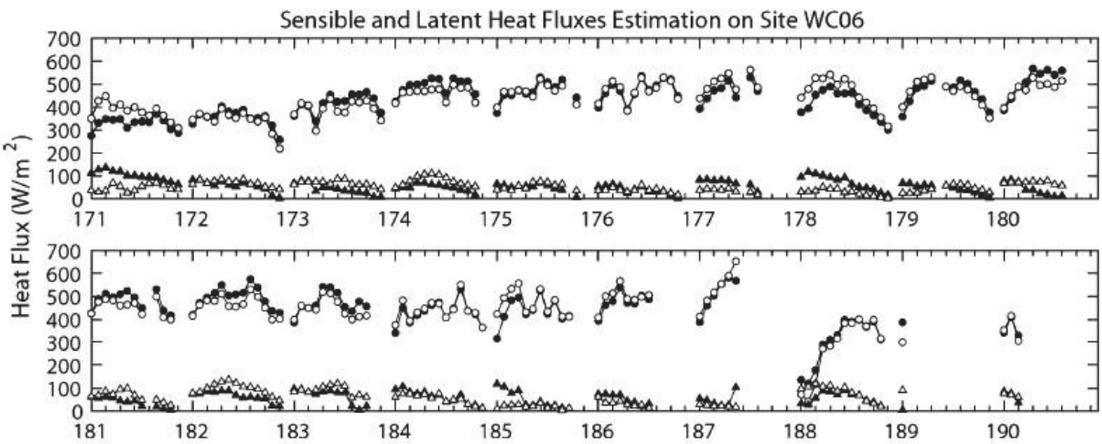

Fig. 4. Reproduction of surface flux development with a one-source model (SEBS) (after Kalma, 2008)

4.2 Two-source SEB models

The equations 10 and 13 make no difference between evaporation soil surface and transpiration from the vegetation and from this reason the resistances are not well defined.

To solve this problem two-source models have been developed for use with incomplete canopies (e.g. Lhomme et al. 1994; Norman et al. 1995; Jupp et al. 1998; Kustas and Norman 1999). These models consider the evaporation as the sum of evaporation from the soil surface and transpiration from vegetation. For example, Norman et. Al. (1995) developed a two-source model (TSM) based on single-time observations which eliminate the need for r_{ex} as used in equations 13 and 14. They reformulated the equation 10 as:

$$H = \rho C_p \frac{T_{rad}(\theta) - T_a}{r_r} \tag{15}$$

where: T_{rad} = directional radiometric surface temperature obtained at zenith view angle θ; r_r = radiometric-convective resistance (s m^{-1}). The radiometric convective resistance is calculated according to the following formula:

$$r_r = \frac{T_{rad}(\theta) - T_a}{\left[\frac{(T_c - T_a)}{r_a} + \left(\frac{(T_s - T_a)}{r_a + r_s}\right)\right]} \tag{16}$$

where: T_c = canopy temperature; T_s = soil surface temperature; R_s = soil resistance to heat transfer (s m^{-1}). To estimate the T_c and T_s variables, Norman et al. used fractional vegetation cover (fc) which depends on sensor view angle (Eq. 17):

$$T_{rad}(\theta) \approx \left[f_c(\theta) T_c^4 + \{1 - f_c(\theta)\} T_s^4\right]^{\frac{1}{4}} \tag{17}$$

H variable is divided in vegetated canopy (H_c) and soil (H_s) influencing the temperature in the canopy air-space. Other revisions of TSM compared flux estimates from two TSM versions proved that thermal imagery was used to constrain T_{rad} and H and microwave remote sensing was employed to constrain near surface soil moisture. The estimations resulting from those two models were compared with flux tower observations. The results showed opposing biases for the two versions that it proves a combination between microwave and thermal remote sensing constraints on H and λE fluxes from soil and canopy. Compared to other types of remote sensing ET formulations, dual-source energy balance models have been shown to be robust for a wide range of landscape and hydro-meteorological conditions.

5. Spatial variability methods using vegetation indices

Visible, near-infrared and thermal satellite data has been used to develop a range of vegetation indices which have been related to land cover, crop density, biomass or other vegetation characteristics (McVicar and Jupp 1998). Several vegetation indices as the Normalized Difference Vegetation Index (NDVI), the Soil Adjusted Vegetation Index (SAVI), the Enhanced Vegetation Index (EVI) and the Simple Ratio (SR), are indicators of canopy greenness which can be related to physiological processes such as transpiration and photosynthesis (Glenn et al., 2007).

5.1 Vegetation indices, reflectance and surface temperature

The SEBAL approach used remotely sensed surface temperature, surface reflectivity and NDVI data. It has been developed for the regional scale and it requires few ground level observations from within the scene. K↓ and L↓ are computed using a constant atmospheric

transmissivity, an appropriate atmospheric emissivity value and an empirical function of T_a, respectively. G is calculated as a fraction of R_n depending on T_{rad}, NDVI and α (Bastiaanssen 2000). The instantaneous values of sensible heat flux are calculated in three main steps. First step makes the difference between T_{ad} and T_{rad} and assumes that the relationship between T_{rad} and the near-surface temperature gradient ($\Delta T = T_{ad} - T_a$) is quasi-linear. Therefore wet and dry extremes can be identified from the image. These extremes fix the quasi-linear relationship relating ΔT to T_{rad}, allowing ΔT to be estimated for any T_{rad} across the image. In the second step, a scatter plot is obtained for all pixels in the entire image of broadband α values versus T_{rad}. Low temperature and low reflectance values correspond to pixels with large evaporation rates, while high surface temperatures and high reflectance values correspond to the areas with little or no evaporation rates. Scatter plots for large heterogeneous regions frequently show an ascending branch controlled by moisture availability and evaporation rate, and a radiation-controlled descending branch where evaporation rate is negligible. The ascending branch indicates that the temperatures increase with increasing α values as water availability is reduced and evaporation rate becomes more limited. For the descending branch the increasing of α induce a decreasing of surface temperature. If the radiation-controlled descending branch is well defined, r_a may be obtained from the (negative) slope of the reflectance–surface temperature relationship. The last step use the local surface roughness (z_{om}) based on the NDVI; is assumed that the z_{om}/z_{oh} ratio has a fix value and H can be calculated for every pixel with λE as the residual term in Eq. 1. The SEBAL models have been used widely with satellite data in the case of relatively flat landscapes with and without irrigation.

The Mapping EvapoTranspiration with high Resolution and Internalized Calibration (METRIC) models, derived from SEBAL are used for irrigated crops (Allen et al. 2007a, b). METRIC model derive ET from remotely sensed data (LANDSAT TM) in the visible, near-infrared and thermal infrared spectral regions along with ground-based wind speed and near surface dew point temperature. In this case extreme pixels are identified with the cool/wet extreme comparable to a reference crop, the evaporation rates being computed wit Penman-Monteith method. The ET from warm/dry pixel is calculated using soil water budget having local meteorological data as input parameters. METRIC model can be used to produce high quality and accurate maps of ET for areas smaller than a few hundred kilometers in scale and at high resolution (Fig. 5). In their study, Boegh et al. (1999) presented an energy balance method for estimating transpiration rates from sparse canopies based on net radiation absorbed by the vegetation and the sensible heat flux between the leaves and the air within the canopy. The net radiation absorbed by the vegetation is estimated using remote sensing and regular meteorological data by merging conventional method for estimation of the land surface net radiation with a ground-calibrated function of NDVI.

SEBAL and METRIC methods assume that the temperature difference between the land surface and the air (near-surface temperature difference) varies linearly with land surface temperature. Bastiaanssen et al. (1998) and Allen and al. (2007) derive this relationship based on two anchor pixels known as the hot and cold pixels, representing dry and bare agricultural fields and wet and well-vegetated fields, respectively. Both methods use the linear relationship between the near-surface temperature difference and the land surface temperature to estimate the sensible heat flux which varies as a function of the near-surface temperature difference, by assuming that the hot pixel experiences no latent heat, i.e., ET = 0.0, whereas the cold pixel achieves maximum ET.

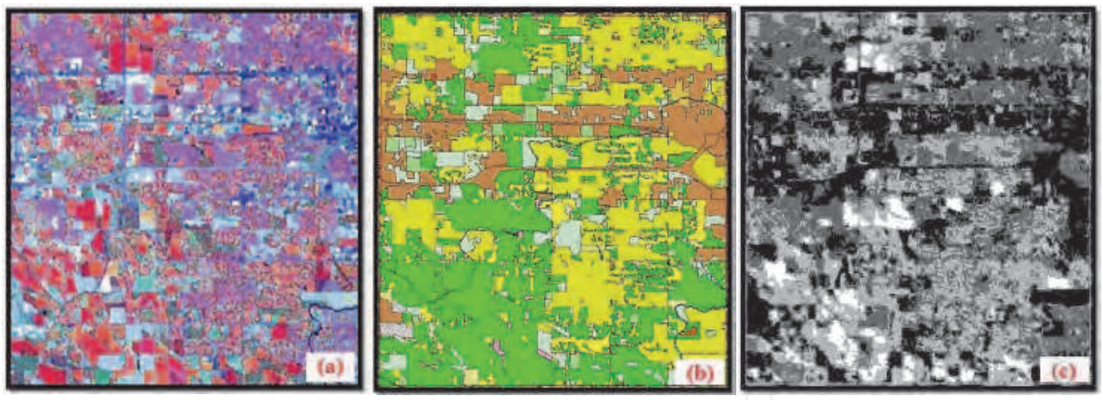

Fig. 5. (a) Landsat color infrared image of T3NR1E of the Boise Valley; (b) Land use/land cover polygons in T3NR1E of the Boise Valley; (c) ET image of T3NR1E the Boise Valley (after R.G. Allen et al., 2007)

The sensible heat flux is assessed like a linear function of the temperature difference between vegetation and mean canopy air stream. The surface temperature recorded by satellite comprises information from soil and from vegetation; therefore the vegetation temperature is estimated taking into account the linear relationship between NDVI and surface temperature. The difference between the surface temperature and the mean canopy air stream temperature is linearly related to the difference between surface temperature and the air temperature above the canopy with the slope coefficient which depend on the canopy structure. This relationship was used to evaluate the mean canopy air stream temperature. The method was used in the Sahel region for agricultural crops, natural vegetation, forest vegetation, with ground based, airborne and satellite remote sensing data and validated with sapflow and latent heat flux measurements. Agreement between remote sensing based estimates and ground based measurements of λE rates is estimated to be better than 30–40 W m^{-2}.

5.2 Reflectance and surface temperature

The Simplified Surface Energy Balance Index (S-SEBI) proposed by Roerink et al. (2000) estimate the instantaneous latent heat flux (λE_i) with (Kalma, 2008):

$$\lambda E_i = \Lambda_i (R_{ni} - G_i) \tag{18}$$

where: (R_{ni} – G_i) = available energy at the time of the satellite overpass; Λ_i = the evaporative fraction. The S-SEBI algorithm has two limitations: the atmospheric conditions have to be almost constant across the image and the image has to contain borh dry and wet areas. Λ_i was obtained from a scatter plot of observed surface temperature (T_{rad}) and Landsat TM derived broadband a values across the single scene. Λ_i is with:

$$\Lambda_i = \frac{T_H - T_{rad}}{T_H - T_{rad}} \tag{19}$$

where: T_{rad} = observed surface temperature for a given pixel; T_H = temperature for the upper boundary (dry radiation controlled conditions - all radiation is used for surface heating and α decreases with increasing surface temperature (T_H - where λE = 0 (W m^{-2})); $T_{\lambda E}$ = temperature at the lower boundary (evaporation controlled wet conditions - all energy

is used for λE and α increases with an increase of surface temperature ($T_{\lambda E}$ -where H = 0 W m^{-2})). This method does not need any additional meteorological data.

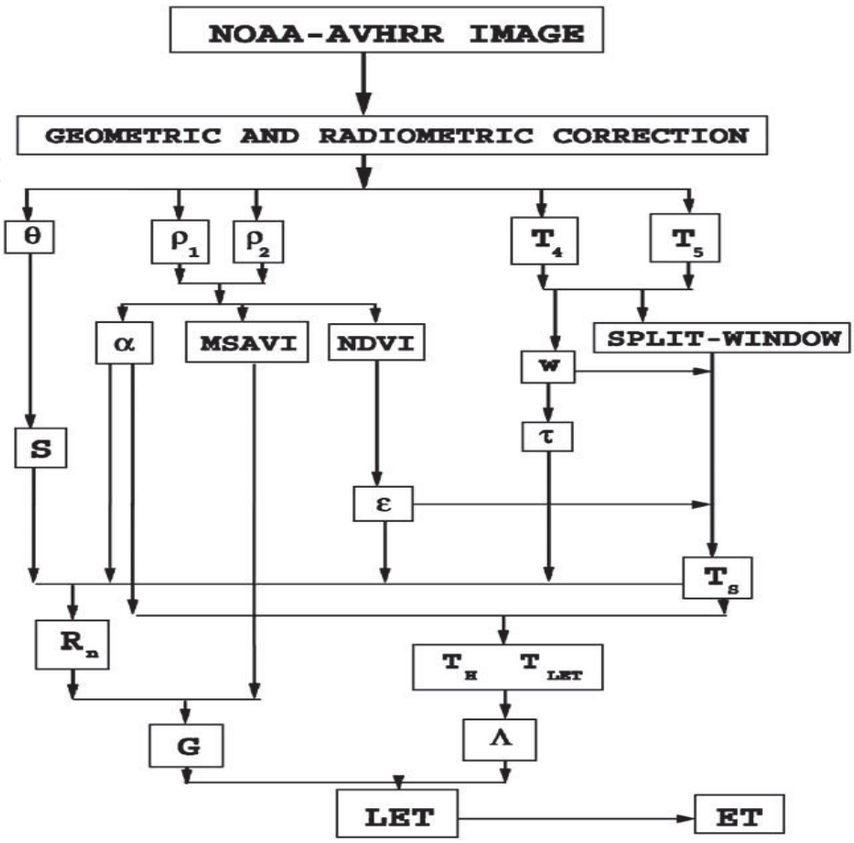

Fig. 6. Flowchart of the proposed methodology to obtain ET from NOAA–AVHRR data (after Sobrino et al., 2007)

Sobrino et. al (2007) use S-SEBI algorithm to estimate the daily evapotranspiration from NOAA-AVHRR images for the Iberian Penisnula. The Figure 6 present the flowchart used by Sobrino et al. (2007) to obtain ET from NOAA-AVHRR. Daily evapotranspiration (ET_d) is given by:

$$ET_d = \frac{\Lambda_i C_{di} R_{ni}}{L} \tag{20}$$

where: R_{nd} = daily net radiation; R_{ni} = instantaneous net radiation: L = 2.45 MJ kg^{-1} = latent heat vaporization; $C_{di}=R_{nd}/R_{ni}$. In this case the daily ground heat flux was considered close to 0. There are several studies which proposed methods for C_{di} calculation. For example Seguin and Itier (1983) proposed a constant value for C_{di} = (0.30±0.03). Wassenaar et al. (2002) showed that this ratio have a seasonal variation 0.05 in winter to 0.3 in summer, following a sine law. In the Sobrino et al. (2007) study, C_{di} was calculated using net radiation fluxes measured at the meteorological station of located on the East coast of the Iberian Peninsula (El Saler area). The ET estimation from high spectral and spatial resolution data (~5 m) was adapted to the low resolution data NOAA-AVHRR (1 km spatial resolution) based on the evaporative fraction concept proposed by Roerink et al. (2007). The main

advantage of the Sobrino et al. (2007) methodology is that the method requires only satellite data to estimate ET.

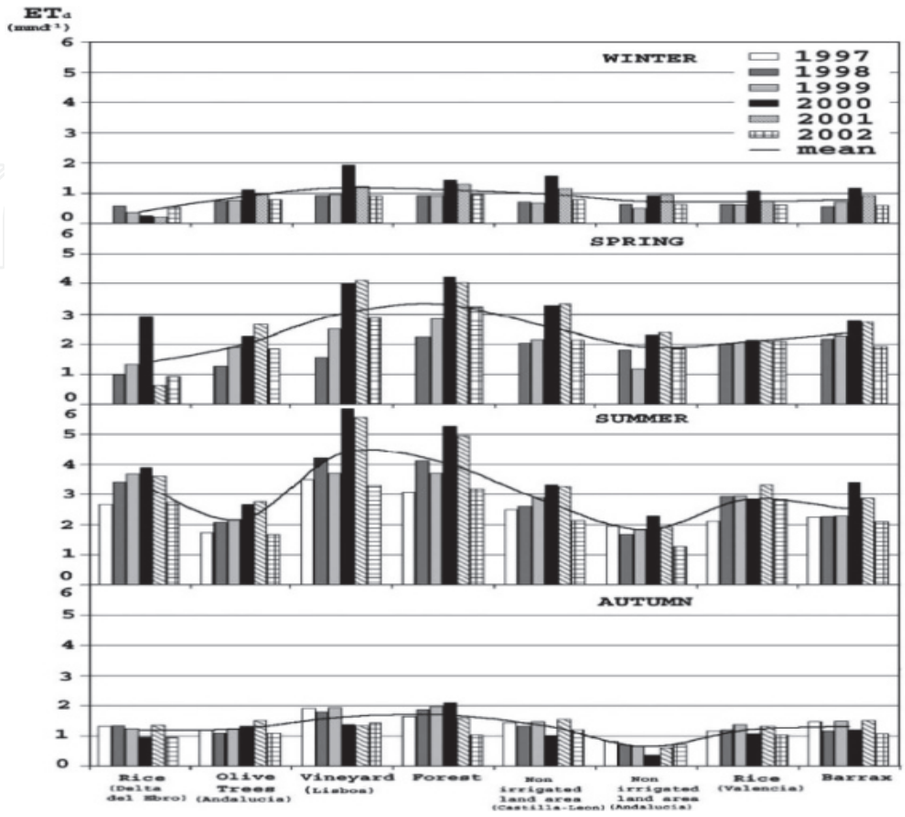

Fig. 7. Monthly evolution (from June 1997 to November 2002) of the daily evapotranspiration (ET_d) in the eight selected zones. There is represented also the temporal mean for the six years of analyzing (after Sobrino et al., 2007).

Its major disadvantage is represented by the requiring that satellite images must have extreme surface temperatures. The method was tested over agricultural area using high resolution values, with errors lower than 1.4 mm d^{-1}. As it can be observed from Fig. 7, regarding the monthly and seasonal evolution of ET the highest values (~6 mm d^{-1}) were obtained in the West of the Iberian Peninsula, which is the most vegetated area. Taking into account the impact of incoming solar energy the higher values of ET was obtained in spring and summer and the lower values in autumn and winter. Seasonal ET was obtained by averaging daily ET over the season. Figure 8 shows as an example the monthly ET maps obtained from the NOAA-AVHRR images acquired in 1999. Fig. 9 also indicates that the highest ET values were obtained in the summer and spring, in the north and west of Iberian Peninsula. To map land surface fluxes and surface cover and surface soil moisture, Gillies and Carlson (1995) combined two model, SVAT and ABL and run it for vegetative cover with the maximum known NDVI and for bare soil conditions with the minimum known NDVI in the scene for a range of soil moisture values until AVHRR observed (T_{rad}) and simulated (T_{ad}) surface temperatures corrected, at which stage the actual fractional vegetation cover (f_c) and surface soil moisture were estimated.

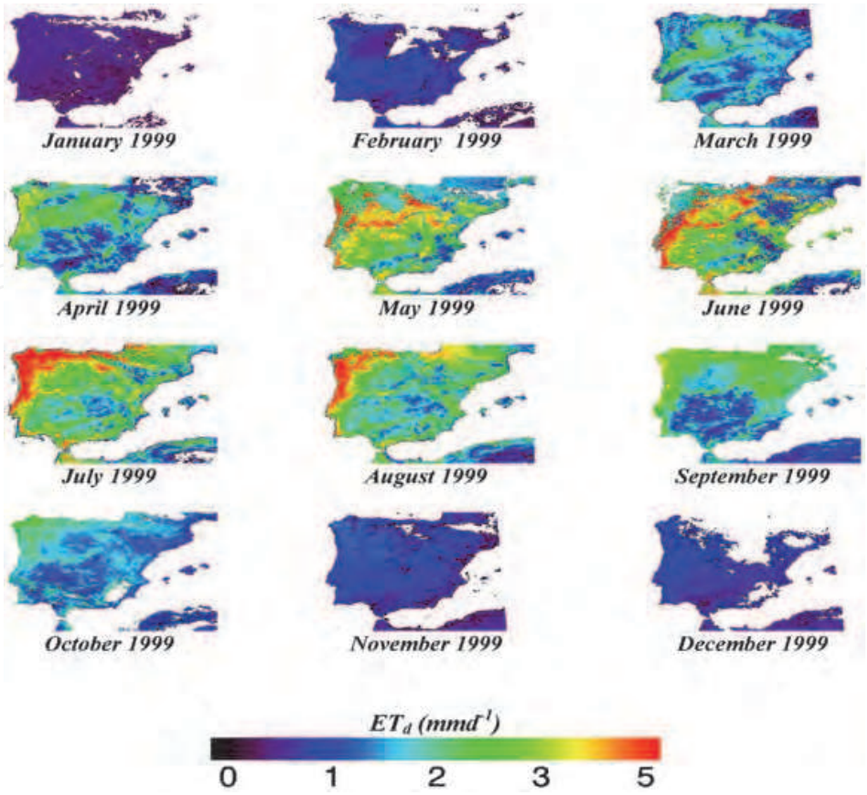

Fig. 8. Monthly mean for the daily evapotranspiration obtained from NOAA–AVHRR data over the Iberian Peninsula in 1999. Pixels in black color correspond to sea and cloud masks and red correspond to higher value of ET (after Sobrino et al., 2007).

5.3 Vegetation indices and surface temperature

Several studies shown the efficiency of ''triangle method'' (Carlson et al. (1995a, b); Gillies et al. 1997; Carlson 2007) to estimate soil moisture from the NDVI–T_{rad} relationship. The major advantages of the remotely sensed VI-T_s triangle method are that: the method allows an accurate estimation of regional ET with no auxiliary atmospheric or ground data besides the remotely sensed surface temperature and vegetation indices; is relatively insensitive to the correction of atmospheric effects. Its limitations are: determination of the dry and wet edges requires a certain degree of subjectivity; to make certain that the dry and wet limits exist in the VI-T_{rad} triangle space most of pixels over a flat area with a wide range of soil wetness and fractional vegetation cover are required. So, the boundaries of this triangle are limiting conditions for H and λE. Other studies suggest the dependence of T_{rad} variability on the remote sending data resolution, thus higher resolution data means that the variations of T_{rad} and NDVI is more related to the land cover type. Lower resolution data show the dependency of the NDVI and T_{rad} variations to agricultural practices and rainfall. Jiang and Islam (2001) proposed a triangle method based on the interpolation of the Priestley–Taylor method (Priestley and Taylor, 1972) using the triangular (T_{rad}, NDVI) spatial variation. The Priestley–Taylor expression for equilibrium evaporation from a wet surface under conditions of minimal advection (λE_{PT}) is given by:

$$\lambda E_{PT} = \alpha_{PT}(R_n - G)\frac{\Delta}{\Delta+\gamma} \tag{21}$$

where: Δ = slope of the saturated vapour pressure curve at the prevailing Ta ((Pa K^{-1}); γ = psychrometric constant (Pa K^{-1}); α_{PT} = Priestley-Taylor parameter defined as the ratio between actual E and equilibrium E. For wet land surface conditions, α_{PT} = 1.26. Its value is affected by global changes in air temperature, humidity, radiation and wind speed. Jiang and Islam (2001) replaced α_{PT} with parameter ϕ which varies for a wide range of r_a and r_c values. The warm edge of the (T_{rad}, NDVI) scatter plot represents pixels with the highest T_{rad} and minimum evaporation from the bare soil component, while E_a can vary function of the vegetation type. Linear interpolation between the sides of the triangular distribution of T_{rad} - NDVI allows to derive ϕ for each pixel using the spatial context of remotely sensed T_{rad} and NDVI. The ϕ values are related to surface wetness, r_s and T_{rad}. Therefore, the minimum value of ϕ is 0 for the driest bare soil pixel and the maximum value is 1.26 for a densely vegetated, well-watered pixel. Thus the actual ϕ value for each pixel in a specified NDVI interval is obtained from the observed $(T_{rad})_{obs}$ with the following:

$$\phi = \phi_{max} \frac{(T_{rad})_{max} - (T_{rad})_{obs}}{(T_{rad})_{max} - (T_{rad})_{min}} \tag{22}$$

where $(T_{rad})_{min}$ and $(T_{rad})_{max}$ are the lowest and highest surface temperatures for each NDVI class, corresponding to the highest and lowest evaporation rates, respectively. The evaporative fraction can be calculated with:

$$\Lambda = \phi \frac{\Delta}{\Delta + \Upsilon} \tag{23}$$

Based on the Jiang and Islam (2001) approach, Wang et al. (2006) obtained better results using the spatial variation (ΔT_{rad}, NDVI), where ΔT_{rad} represent the day–night difference in T_{rad}, obtained from MODIS data. However, to convert Λ into E, the method described above still requires estimation/ measurement of net radiation (R_n) and soil heat flux (G). In a later work, Jiang and Islam (2003) consider the fractional vegetative cover (f_c) as a more suitable generalized vegetation index calculated from the normalized NDVI with (Kalma et al. 2008):

$$f_c = \left(\frac{NDVI - NDVI_{min}}{NDVI_{max} - NDVI_{min}} \right)^2 \tag{24}$$

They assumed that the evaporative fraction Λ = λE/(R_n - G) is linearly related to ΔT = T_{rad} - T_a, inside a certain class f_c. The reason for this assumption is that theΔT is more representative for sensible heat flux H. Thus the evaporative fraction can be estimated from f_c and ΔT, for a given set of ΔT_{max}, ΔT_e ($\Delta T_e = \Delta T_{max}$ for f_c = 1) and a stress factor (β). In their study, they used NOAA-AVHRR data and obtained better results using the aerodynamic resistance-energy balance method represented by Eq. 13, this equation including atmospheric stability corrections and using an iterative procedure to reach the most appropriate kB^{-1} value.

Serban et al. (2010) used the Priestly-Taylor equation modified by Jiang and Islam (2001) in their study to estimate the evapotranspiration using remote sensing data and Grid Computing. The most advantage of Priestly-Taylor equation is that the all terms can be calculated using remotely sensed data. Grid computation procedure has two major advantages: strong data processing capacity and the capability to use distributed computing resources to process the spatial data offered by a satellite image. According to Jiang and Islam (2001) the parameter α_{PT} parameter is obtained by two-step linear interpolation: in the

first step is obtained upper and lower bounds of α_{PT} for each specific NDVI class (determined from the land use/land cover map); in the second step the parameter α_{PT} is ranged within each NDVI class between the lowest temperature pixel and the highest temperature pixel. According to land use/land cover map, for this paper, was considered four main land uses: vegetation, water, barren land and urban. Each NDVI value corresponds to a certain NDVI class. In this case the relationship between LST and NDVI is used. Thus, the parameter α_{PT} is calculated with:

$$\alpha_{PT} = \left(\frac{\Delta + \gamma}{\Delta}\right)\left(\frac{LST_i^{max} - LST}{LST_i^{max} - LST_i^{min}}\right)\left(\frac{NDVI_i^{max} - NDVI_i^{min}}{NDVI_i^{max}}\right) + \left(\frac{\Delta + \gamma}{\Delta}\right)\left(\frac{NDVI_i^{min}}{NDVI_i^{max}}\right) \quad (25)$$

where: LST = surface temperature for current pixel; LST_i^{max} and LST_i^{min} = maximum and minimum surface temperature within NDVI class which has the current pixel; $NDVI_i^{max}$ and $NDVI_i^{min}$ are the maximum and minimum NDVI within NDVI class which has the current pixel. They calculated the daily value of ET with the following (Fig. 9):

$$\lambda E_{daily} = \alpha_{PT} \frac{2DL(R_i - G_i)}{\pi sin\left(\pi \frac{t}{DL}\right)} \quad (26)$$

where: DL = total day length (hours); t = time beginning at sunrise. To obtain the 24 hours totals, the daily ET values are multiplied by 1.1 for all days. LST was computed using Jimenez- Munoz and Sobrino's algorithm which requires a single ground data (the total atmospheric water vapor content – w) (Fig. 10):

$$LST = \gamma[LSE^{-1}(\psi_1 L_{sensor} + \psi_2) + \psi_3] + \delta \quad (27)$$

$$\gamma = \left[\frac{c^2 L_{sensor}}{T_{sensor}^2}\left(\frac{\lambda^4}{c_1} L_{sensor} + \lambda^{-1}\right)\right] \quad (28)$$

$$\delta = \gamma L_{sensor} + T_{sensor} \quad (29)$$

$$L_{sensor} = gain * DN + bias - spectral\ radiance \quad (30)$$

$$T_{sensor} = \frac{K_2}{ln\left(\frac{K_1}{L_{sensor}} + 1\right)} \quad (31)$$

where: LSE = land surface emissivity = 1.0094+0.047*ln(NDVI); λ = effective wavelength; DN = digital number of a pixel; T_{sesnor} = brightness temperature; c^1 = 1.19104*10^8 Wμm^4 m^{-2}sr^{-1}; c^2 = 14387.7μmK; ψ_i (i = 1, 2, 3) = atmospheric parameters, which depend on total atmospheric water vapor content (w). Besides satellite data, this study uses two ground meteorological data: the total atmospheric water vapor content - w, used in LST estimation algorithm, and the air temperature - T_{air}. To estimate evapotranspiration, Serban et al. (2010) used one subset of Landsat ETM+ (7th June 2000) for Dobrogea area corresponding to Constanta weather station, which was atmospherically corrected.

From the bands ETM+ 3 and 4 were analyzed the NDVI values, the band ETM+ 6 was processed to determine LST, and the other bands (ETM+ 1, 2, 5 and 7) were used to estimate the albedo values. The difference between the actual mean soil surface temperature at the

time when satellite passed and the remote sensed mean land surface temperature (0.73^{O}C) is considered acceptable. The evapotranspiration (Fig. 10) ranges between 0.33 and 5.24mm/day. According to Constanta weather station, the multi-annual average of the evapotranspiration in June is between 4.5 and 5.6 mm/day, so the estimation error is eligible.

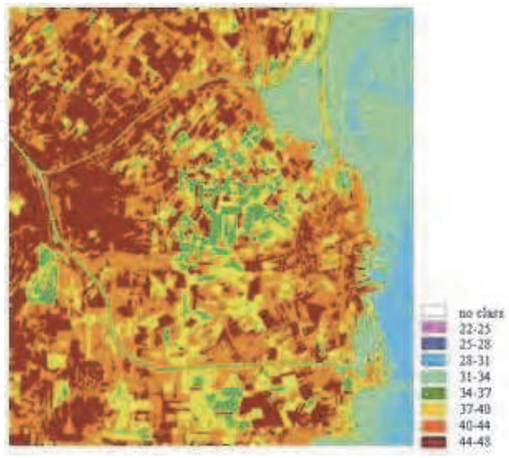

Fig. 9. LST Image - Dobrogea region, 2000 (After Serban et al., 2010)

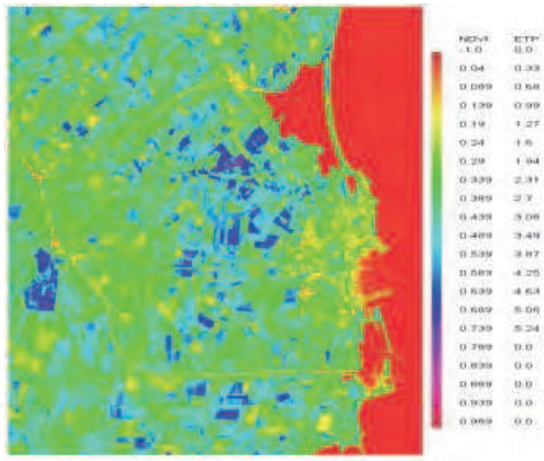

Fig. 10. ETP Image - Dobrogea region, 2000 (After Serban et al., 2010)

6. ET estimation using meteorological data

6.1 Crop evapotranspiration

At a crop level, ET may not occur uniformly because variations in crop germination, soil water availability, and other factors such as non-uniform water and nutrient applications and an uneven distribution of solar radiation within the canopy. Usually, the top leaves are more active in transpiration than the lower leaves because they receive more light. Also, the bottom leaves mature and age earlier and they may have lower transpiration rates than the greener and younger top leaves. Thus, weather parameters, crop characteristics, environmental and management aspects are the factors which influence the evaporation and transpiration

processes. The main weather parameters influencing evapotranspiration are radiation, air temperature, humidity and wind speed. Several algorithms have been developed to estimate the evaporation rate from these parameters. The evaporation power of the atmosphere is expressed by the reference crop evapotranspiration (ET_o) which represents the evapotranspiration from a standardized vegetated surface (Allen et al., 1998). The reference surface is a hypothetical grass reference crop with specific characteristics. Because ET_o is affected by only climatic parameters, it is a climatic parameter and may be computed from weather data. Thus ET_o is the evaporating power of the atmosphere at a specific location and time of the year and does not take into account the crop characteristics and soil factors.

Crop water requirement is defined as the amount of water required to compensate the evapotranspiration loss from the cropped field. Even the values for crop evapotranspiration are identical with crop water requirement (CWR), crop evapotranspiration refers to the amount of water that is lost by evapotranspiration, while CWR refers to the amount of water that needs to be supplied. Thus, the irrigation water requirement represents the difference between the crop water requirement and effective precipitation and also includes additional water for leaching of salts and to compensate for non-uniformity of water application (Allen et al., 1998). Several empirical methods have been developed over the last five decades in order to estimate the evapotranspiration from different climatic variables. Testing the accuracy of the methods under a new set of conditions is laborious, time-consuming and costly, and yet evapotranspiration data are frequently needed at short notice for project planning or irrigation scheduling design. To meet this need, guidelines were developed and published in the FAO Irrigation and Drainage Paper No. 24 'Crop water requirements'. From different data availability, four methods are usually used to estimate the reference crop evapotranspiration (ET_o): the Blaney-Criddle, radiation, modified Penman and pan evaporation methods. From these four methods, the modified Penman-Monteith method offer the best results with minimum possible error in relation to a living grass reference crop. The radiation method can be used for areas where available climatic data include measured air temperature and sunshine, cloudiness or radiation, but not measured wind speed and air humidity. The Blaney-Criddle method is better to be applying for areas where available climatic data cover air temperature data only. The pan method gives acceptable estimates, depending on the location of the pan. Based on the original Penman- FAO proposed a standard parameterization of the Penman–Monteith method for estimating the evaporation from a -irrigated, homogenous, 0.12 m grass cover considered as a ‘‘reference crop’’ (Allen et al., 1998) (Fig. 11).

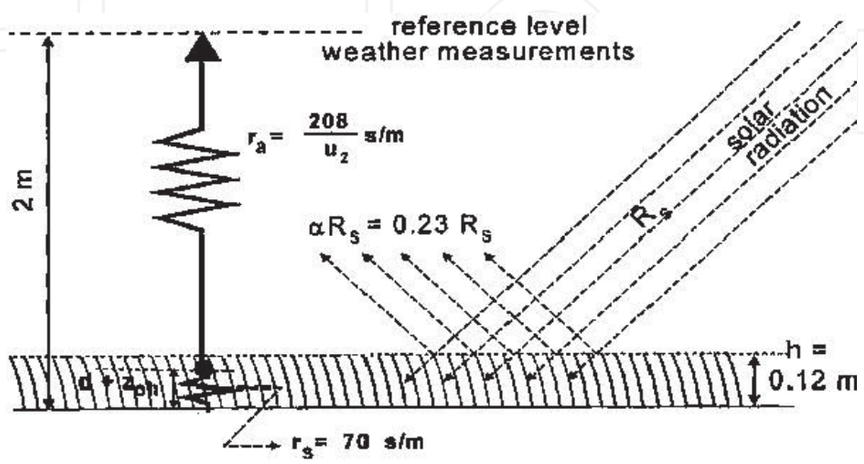

Fig. 11. Characteristics of the hypothetical reference crop (after Allen et al., 1998)

Monteith equation and the equations of the aerodynamic and surface resistance, the FAO Penman-Monteith method to estimate ET_o is the following:

$$ET_0 = \frac{0.408\Delta(R_n - G) + \gamma\left(\frac{900}{T+273}\right)u_2(e_s - e_a)}{\Delta + \gamma(1 + 0.34u_2)} \quad (32)$$

where: ET_0 = reference evapotranspiration [mm day^{-1}]; R_n = net radiation at the crop surface [MJ m^{-2} day^{-1}]; G = soil heat flux density [MJ m^{-2} day^{-1}]; T = mean daily air temperature at 2 m height [°C]; u_2 = wind speed at 2 m height [m s^{-1}]; e_s = saturation vapour pressure [kPa]; e_a = actual vapour pressure [kPa]l; e_s - e_a = saturation vapour pressure deficit [kPa]; Δ = slope vapour pressure curve [kPa °C^{-1}]; γ = psychrometric constant [kPa °C^{-1}]. The equation uses standard climatological records of solar radiation (sunshine), air temperature, humidity and wind speed. To obtain correct estimations of ET_0, the weather measurements should be made at 2 m (or converted to that height) above an extensive surface of green grass, shading the ground and not short of water. The psychrometric constant, γ, is calculated with:

$$\gamma = \frac{C_p P}{\varepsilon\lambda} = 0.665 * 10^{-3} \quad (33)$$

Where: P = atmospheric pressure [kPa]; λ = latent heat of vaporization, 2.45 [MJ kg^{-1}]; c_p = specific heat at constant pressure, 1.013 10-3 [MJ kg^{-1} °C^{-1}]; ε = ratio molecular weight of water vapour/dry air = 0.622. For standardization, T_{mean} for 24 hour is defined as the mean of the daily maximum (T_{max}) and minimum temperatures (T_{min}) rather than as the average of hourly temperature measurements.

$$T_{mean} = \frac{T_{max} - T_{min}}{2} \quad (34)$$

The temperature is given in degrees Celsius (°C), Fahrenheit (°F) or in Kelvin (K =C° + 273,16).

$$P = 101.3\left(\frac{293 - 0.0065z}{293}\right)^{526} \quad (35)$$

where: z = elevation above sea level [m].

6.2 CROPWAT model

CROPWAT is a decision support system developed by the Land and Water Development Division of FAO for planning and management of irrigation. The main functions of CROPWAT model are: to calculate the reference evapotranspiration, crop water requirements and crop irrigation requirements; to develop irrigation schedules under different management conditions and water supply schemes; to estimate the rainfed production and drought effects; to evaluate the efficiency of irrigation practices.

The input data of the model are the following climatic, crop and soil data: reference crop evapotranspiration: (ET_o) values measured or calculated using the FAO Penman–Montieth equation based on monthly climatic average data of the minimum and maximum air temperature (°C), relative humidity (%), sunshine duration (h) and wind speed (m/s); rainfall data: (daily/monthly data); monthly rainfall is divided for each month into a number of rainstorms; a cropping pattern: crop type, planting date, crop coefficient data files (including K_c values, stage days, root depth, depletion fraction, K_y values) and the area planted (0– 100% of the total area); a set of typical crop coefficient data files are provided in the program; soil type: total available soil moisture, maximum rain infiltration rate,

maximum rooting depth, and initial soil moisture depletion (% of the total available moisture);scheduling criteria: several options can be selected regarding the calculation of the application timing and application depth.
The output parameters for each crop are crop reference crop evapotranspiration Et_0 (mm/period), crop K_c (average values of crop coefficient for each time step, effective rain (mm/period) (the amount of water that enters in the soil); water requirements (CWR) or ET_m (mm/period); irrigation requirements (IWR - mm/period); actual crop evapotranspiration (ET_c - mm); effective rain (mm/period) which represents the amount of water that enters into the soil; daily soil moisture deficit (mm); estimated yields reduction due to crop stress (when ET_c/ET_m falls below 100%).
The CROPWAT model can compute the actual evapotranspiration using the FAO Penman–Monteith equation or using directly the evapotranspiration measurements values. The crop water requirements (CWR) or maximum evapotranspiration (ET_m) (mm/period) are calculated as:

$$CWR = ET_0 * CropK_c \tag{36}$$

This means that the peak CWR in mm/day can be less than the peak Et_o value when less than 100% of the area is planted in the cropping pattern.
The average values of the crop coefficient (K_c) for each time step are estimated by linear interpolation between the K_c values for each crop development stage. The ''Crop K_c" values are calculated as:

$$CropK_c = K_c * CropArea \tag{37}$$

where CropArea is the area covered by the crop. So, if the crop covers only 50% of the area, the "Crop Kc" values will be half of the Kc values in the crop coefficient data file.
The CROPWAT model operates in two modes: computing the actual evapotranspiration using climatic parameters and using directly the evapotranspiration measurements values.
Possibilities to use the satellite-based data as input into the CROPWAT model are limited, because this model was not developed to use satellite-derived information directly. But this information can be useful for the comparison/validation procedures of some model input/output data, as precipitation, sunshine duration and evapotranspiration. Satellite based data can be used by CROPWAT model in different ways: measured evapotranspiration may be replaced with estimations derived from satellite data; for comparison and validation procedures; satellite-derived evapotranspiration values may bring better accuracy for the specialization of the punctual computing values; satellite information may be used for the assessment of the some reference parameters of the actual evapotranspiration (e.g. Land surface temperature, vegetation indexes, etc.).

6.3 Using earth observation data and CROPWAT model to estimate the actual crop evapotranspiration

There is a strong dependence between evapotranspiration and surface temperature on the, thus thermal images meteorological satellites (METEOSAT, NOAA, MODIS, LANDSAT) adequate for mapping of regional evapotranspiration. Several works have been done to determine regional evapotranspiration from satellite data (Batra et al., 2006; Courault et al., 2005; Wood et al., 2003). The application of NOAA AVHRR data seems to be more successful because of the higher spatial and spectral resolution (Stancalie et al., 2010). Multichannel algorithms are routinely used for atmospheric correction of the AVHRR data.

Efforts are directed towards the estimation of surface temperatures by considering the effects of emissivity (Lagouarde and Brunet, 1991; Li and Becker, 1993). The method used for the estimation of the daily crop actual evapotranspiration, ET_{cj}, is based on the energy balance of the surface. The method uses the connection between evapotranspiration, net radiation and the difference between surface and air temperatures measured around 14:00 h (the time of the satellite passage), local time. The first version of the method used a simplified linear relationship as:

$$ET_{cj} - R_{nj} = A - B * (T_s - T_{amax}) \quad (38)$$

where R_{nj} is the daily net radiation; T_s and T_{amax} is the surface and air maximum temperature; A, B are coefficients which depend on the surface type and the daily mean wind speed. Coefficients A and B may be determined either analytically, on the basis of the relationships given by Lagouarde and Brunet (1991), or statistically. The coefficients A and B are stable in the case of mature crop vegetation cover and in clear sky conditions. The coefficient B vary considerably, function of the land vegetation cover percent. In case of soil with great thermal inertia, the heat flux changed by conduction at the soil-atmosphere interface can be neglected and the computing relationship for daily actual crop evapotranspiration can be expressed in a version 2 of the proposed method:

$$ET_{cj} = R_{nj} - B' * (T_s - T_{amax}) \quad (39)$$

$$B' = 0.0253 + \left[\frac{1.0016}{log2(2/zh)}\right] v \quad (40)$$

$$zh = [1 - exp(-LAI)]\left[exp\left(-\frac{LAI}{2}\right)\right] \quad (41)$$

where: v = daily average wind speed; zh = vegetation roughness and LAI the foliar index.
One possible use of satellite information is to replace the measured evapotranspiration by estimations made from satellite information. Because the estimations made from satellite information are available only for clear sky conditions, it was not possible to estimate the monthly average evapotranspiration, as input data in the CROPWAT model. For this reason, the satellite-derived data have been used for comparison/validation procedures of the CROPWAT model output data, like evapotranspiration. Fig. 12 presents the comparison between daily crop evapotranspiration values computed by the CROPWAT model and those computed through the energy balance method (Version 1), using remotely sensed data at the Alexandria and Craiova test-areas (situated in the south-western part of Romania), in the conditions of the year 2000 (Stancalie et al., 2010, 2010).
Analysis of model results concerning comparison of daily actual crop evapotranspiration calculated by using climatic data vs. satellite estimations based on the surface energetic balance (Version 1) showed that ET_c values from satellite information are in general higher than those simulated by the model, the differences being from +0.45 - 1.9 mm/day. Preliminary results highlighted a good correlation between the simulated values (CROPWAT) and those derived from the satellite data; with relative errors from +20% - 18% at Craiova site and from +13% -17% at Alexandria site (Stancalie et al., 2010).
Fig. 13 shows a comparison between ET_c simulated daily by the CROPWAT model over the whole maize-growing season and by the energy balance method (Version 2) respectively, using satellite data, at Alexandria and Craiova test-areas. The ET_c calculated by the model is very similar to the estimated one. The results obtained can constitute the premise of an ET_c data validation process, determined by the CROPWAT model (Stancalie et al., 2010).

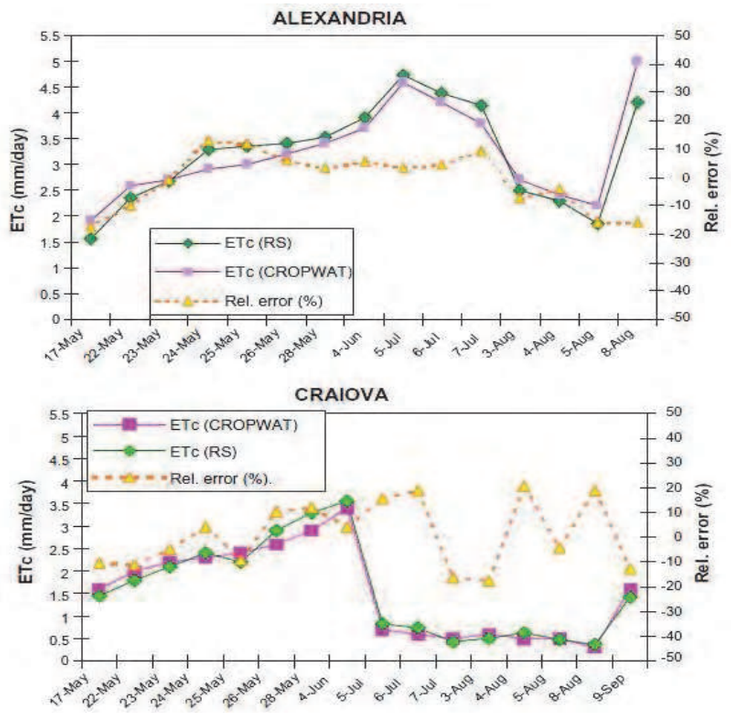

Fig. 12. Comparison between daily crop evapotranspiration values computed by the CROPWAT model and by the energy balance method (Version 1) using satellite data at the Alexandria and Craiova test-areas (after Stancalie et al., 2010)

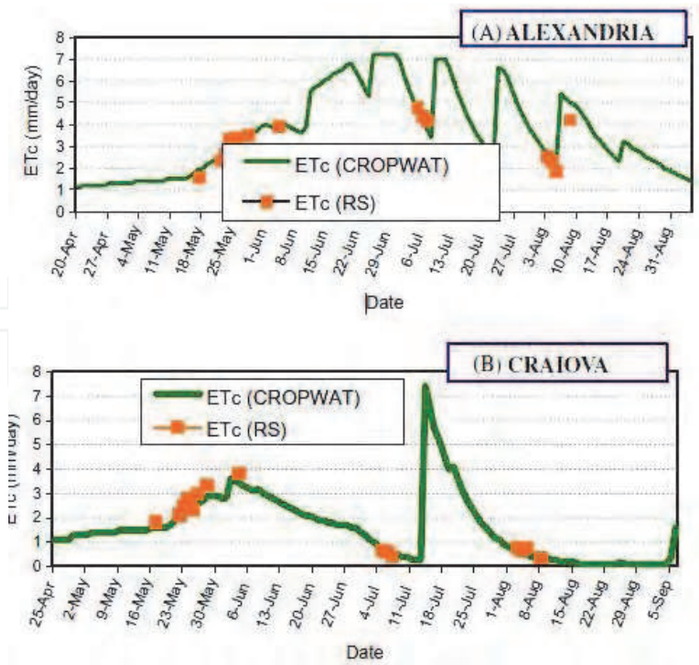

Fig. 13. Comparison between daily crop et values computed by the CROPWAT model and by the energy balance method (Version 2) using satellite data, at Alexandria (A) and Craiova (B) test-areas, for the maize vegetative development period in 2000 (Stancalie et al., 2010).

7. Conclusions

The use of the multispectral satellite data can improve the classical methods applied in determining the agrometeorological parameters, including evapotranspiration.
Estimating evapotranspiration using remote sensing methodologies have a significant role in irrigation management and crop water demand assessment, for plant growth, carbon and nutrient cycling and for production modeling in dry land agriculture and forestry. Also it can have an important role in catchment hydrology, and larger scale meteorology and climatology applications. In the last years, due to the exceptional developments of satellite technology, a wide range of remote sensing-based evapotranspiration (ET) methods/models have been developed and evaluated. The use of remote sensing data for ET estimation is mainly based on land surface temperature (LST) and reflectivity (using different spectral regions) due to satellite ability to spatially integrate over heterogeneous surfaces at a range of resolutions and to routinely generating areal products once long time-series data availability issues are overcome. The chapter reviews some main methods for estimating crop evapotranspiration based on remotely sensed data, and highlights uncertainties and limitations associated with those estimation methods. This paper is focused on Surface Energy Balance models (SEB), spatial variability methods using vegetation indices and ET estimation using meteorological data through CROPWAT model. The analysis and critical issues are supported by the dedicated literature and specific case-studies. This review provides information of temporal and spatial scaling issues associated with the use of optical and thermal remote sensing for estimating evapotranspiration. Improved temporal scaling procedures are required to extrapolate estimates to daily and longer time periods and gap-filling procedures are needed when temporal scaling is affected by intermittent satellite coverage. It is also noted that analysis of multi-resolution data from different satellite/sensor systems is able to assist the development of spatial scaling and aggregation approaches. Approaches differ in: (i) type and spatial extent of application (e.g. irrigation, dry-land agriculture); (ii) type of remote sensing data; and (iii) use of ancillary (micro-) meteorological and land cover data. The integration of remotely sensed data into methods/models of ET facilitates the estimation of water consumption across agricultural regions. There are important limitations for using remote sensing data in estimating evapotranspiration.
Usually evapotranspiration is computed using land surface temperature and air temperatures. All this methods are affected by errors induced by estimation or measurements of those temperatures. The accuracy of T_{rad} observations is influenced by atmospheric factors, surface emissivity or view angle. Emissivity information is useful in estimating of the radiative temperature of the land surface. Several direct methods (which atmospheric variables are coupled with radiative transfer models) or indirect algorithms (use only remote sensing data) to make atmospheric corrections in order to obtain the brightness temperature that represents the temperature of a black body that would have the same radiance as that observed by the radiometer. The uncertainties of surface temperature have a strong influence in determination of sensible heat flux H. The difference between surface and air temperatures depends on many factors, including vegetation type, fractional cover f_c and view angle. Another important limitation of various spatial variability methods is considered the fact according to the highest and lowest surface temperatures observed in the one scene are assumed to represent very dry and very wet pixels. Usually the available energy (R_n - G) is obtained from ground based point observations of R_n: R_n is estimated

based on observations of K↓, α, LAI, emissivity of land surface and atmosphere, and T_{rad}. Such kind of estimation generates errors in the calculation of long and short wave components. G can be estimated for example as function of NDVI. An alternative method would be to assume that soil heat flux is a constant fraction of net radiation flux, but this estimation doesn't take into account the diurnal variation. Many models for ET estimation need ground based meteorological data, mainly air temperature and wind speed. For that models which based on computing the difference between Tad and Ta, the time and location of air temperature (Ta) observations and their spatial representativeness are very important).

Incomplete vegetation cover generates also errors in evapotranspiration estimation. The two source models require parameterizations for the segmentation of the computed surface temperature between vegetation and soil, for the turbulent exchange of heat and mass between soil and atmosphere and between vegetation and atmosphere. Also, these models require some assumptions regarding solar transmittance, extinction coefficients and canopy emissivity in order to compute the variation of net radiation flux inside the canopy.

Another important limitation, regarding the spatial variability methods is that a large number of pixels are required over the area of interest with a wide range of soil wetness and fractional vegetation cover. The identification of vegetation limits for bare soil or full vegetation cover can be easily done using high resolution images which display a wide range in surface wetness conditions and land cover conditions

Remote sensing data is a useful tool that provides input data in land surface model (NDVI, LAI, f_c – fraction cover) and can be used to correct the state variables of the models.

The frequency of spatial resolution imagery is also very significant: satellites which provide high resolution data usually have lower temporal frequency while low spatial resolution images have higher temporal frequency. Some applications require different spatial and temporal coverage rates and need different ''turn-around'' times. If acquiring the satellite data and ET estimation method are more time consuming, the method are not very convenient for operational applications like determining water requirements for irrigated agriculture.

Another significant limitation for using remote sensing is the presence of clouds that generates intermittent coverage. Cloudy days are characterized by a diffuse light, whereas while direct light is dominant on clear days when most TIR data are acquired for use in modeling applications. Most SEB models have been developed for use in cloud-free conditions and do not makes difference between direct and diffuse radiation; they use only daytime data obtained for clear-sky conditions. For a continuously monitoring of water balance, the effects of an increased diffuse fraction should be taking into account, because the diffuse radiation is used by vegetation more efficiently than direct radiation. For water use efficiency, to ignore difference between direct and diffuse radiation can induce significant differences in ET estimations.

8. References

Allen RG, Pereira LS, Raes D, Smith M (1998), Crop evapotranspiration - guidelines for computing crop water requirements. FAO irrigation and drainage paper 56, Rome, Italy http://www.fao.org/docrep/X0490E/X0490E00.htm

Allen RG, Tasumi M, Trezza R (2007a) Satellite-based energy balance for mapping evapotranspiration with internalized calibration (METRIC): model. J Irrig Drain Eng 133(4):380–394. doi:10.1061/(ASCE) 0733-9437(2007)133(4):(380)

Allen RG, Tasumi M, Trezza R (2007b) Satellite-based energy balance for mapping evapotranspiration with internalized calibration (METRIC): applications. ASCE J Irrig Drain Eng 133(4):395–406

Bastiaanssen WGM, Menenti M, Feddes RA, Holtslag AAM (1998a) A remote sensing surface energy balance algorithm for land. I. Formulation. J Hydrol (Amst) 212/213:198–212. doi:10.1016/S0022-1694(98)00253-4

Bastiaanssen WGM (2000) SEBAL-based sensible and latent heat fluxes in the irrigated Gediz Basin, Turkey. J Hydrol (Amst) 229:87–100. doi:10.1016/S0022-1694(99)00202-4

Batra N, Islam S, Venturini V, Bisht G, Jiang L (2006) Estimation and comparison of evapotranspiration from MODIS and AVHRR sensors for clear sky days over the Southern Great Plains. Remote Sens Environ 103:1–15. doi:10.1016/j.rse.2006.02.019

Boegh E, Soegaard H, Hanan N, Kabat P, Lesch L (1999) A remote sensing study of the NDVI–Ts relationship and the transpiration from sparse vegetation in the Sahel based on high-resolution satellite data. Remote Sens Environ 69:224–240. Doi: 10.1016/S0034-4257(99)00025-5

Boegh E, Soegaard H, Thomsen A (2002) Evaluating evapotranspiration rates and surface conditions using Landsat TM to estimate atmospheric resistance and surface resistance. Remote Sens Environ 79:329–343. doi:10.1016/S0034-4257(01)00283-8

Brutsaert W (1999) Aspects of bulk atmospheric boundary layer similarity under free-convective conditions. Rev Geophys 37:439–451. Doi: 10.1029/1999RG900013.

Burba G., Hubart J.A., Pidwirny M. (2010), Evapotranspiration, Encyclopedia of Earth, Eds. Cutler J. Cleveland (Washington, D.C.: Environmental Information Coalition, National Council for Science and the Environment, August 3, 2010, http://www.eoearth.org/article/Evapotranspiration

Carlson TN, Capehart WJ, Gillies RR (1995a) A new look at the simplified method for remote sensing of daily evapotranspiration. Remote Sens Environ 54:161–167. Doi: 10.1016/0034-4257(95)00139-R

Carlson TN (2007) An overview of the ''triangle method'' for estimating surface evapotranspiration and soil moisture from satellite imagery. Sensors 7:1612–1629

Cleugh HA, Leuning R, Mu Q, Running SW (2007) Regional evaporation estimates from flux tower and MODIS satellite data. Remote Sens Environ 106:285–304. doi:10.1016/j.rse.2006.07.007

Courault D, Seguin B, Olioso A (2005) Review on estimation of evapotranspiration from remote sensing data: from empirical to numerical modelling approaches. Irrig Drain Syst 19:223–249. Doi: 10.1007/s10795-005-5186-0

Gillies RR, Carlson TN (1995) Thermal remote sensing of surface soil water content with partial vegetation cover for incorporation into climate models. J Appl Meteorol 34:745–756. doi :10.1175/1520-0450(1995)034\0745:TRSOSS[2.0.CO;2

Gillies RT, Carlson TN, Cui J, Kustas WP, Humes KS (1997) A verification of the ''triangle'' method for obtaining surface soil water content and energy fluxes from remote measurements of the Normalized Difference Vegetation Index (NDVI) and surface

radiant temperatures. Int J Remote Sens 18(15):3145–3166. doi:10.1080/014311697217026

Glenn EP, Huete AR, Nagler PL, Hirschboeck KK, Brown P (2007) Integrating remote sensing and ground methods to estimate evapotranspiration. Crit Rev Plant Sci 26(3):139–168. doi:10.1080/07352680701402503

Hope AS, Petzold DE, Goward SN, Ragan RM (1986) Simulated relationships between spectral reflectance, thermal emissions, and evapotranspiration of a soybean canopy. Water Resour Bull 22:1011–1019

Huntington, T. 2006. Evidence for intensification of the global water cycle: review and synthesis. J Hydr. 319: 83–95.

Hutley, L., O'Grady, A., and Easmus, D. 2001. Monsoonal influences on evapotranspiration of savanna vegetation of northern Austalia. Oecologia 126: 434–443.

Huxman, T., Smith, M., Fay, P., Knapp, A., Shaw, M., Loik, M., Smith, S., Tissue, D., Zak, J., Weltzin, J., Pockman, W., Sala, O., Haddad, B., Harte, J., Koch, G., Schwinning, S., Small, E.,Williams, D. 2004. Convergence across biomes to a common rain-use efficiency. Nature 429: 651–654.

Huxman, T.,Wilcox, B., Breshears, D., Scott, R., Snyder, K., Small, E., Hultine, K., Pockman, W., and Jackson, R. 2005. Ecohydrological implications of woody plant encroachment. Ecology 86: 308–319.

Jacquemin, B.&Noilhan, J. 1990. Sensitivity study and validation of land surface parametrization using the Hapex-Mobilhy data set. Bound-Layer Meteorology 52: 93–134.

Jiang L, Islam S (2001) Estimation of surface evaporation map over southern Great Plains using remote sensing data. Water Resour Res 37:329–340. doi:10.1029/2000WR900255

Jupp DLB, Tian G, McVicar TR, Qin Y, Fuqin L (1998) Soil moisture and drought monitoring using remote sensing I: theoretical background and methods. CSIRO Earth Observation Centre, Canberra http://www.eoc.csiro.au/pubrep/scirpt/jstc1.pdf

Kalma, J. D., McVicar, T. R. and McCabe, M. F. (2008). "Estimating land surface evaporation: A review of methods using remotely sensed surface temperature data." Surveys in Geophysics 29(4-5): 421-469.

Katerji N., Perrier A.1985 - Détermination de la résistance globale d'un couvert végétal à la diffusion de vapeur d'eau et de ses différentes composantes. Approche théorique et vérification expérimentale sur une culture de luzerne. Agric. For Meteorol., 34, 2-3, 105-120.

Kustas WP, Norman JM (1996) Use of remote sensing for evapotranspiration monitoring over land surfaces. Hydrol Sci J 41(4):495–516

Kustas WP, Norman JM (1999) Evaluation of soil and vegetation heat flux predictions using a simple two source model with radiometric temperatures for partial canopy cover. Agric For Meteorol 94:13–29. doi:10.1016/S0168-1923(99)00005-2

Kustas WP, French AN, Hatfield JL, Jackson TJ, Moran MS, Rango A (2003a) Remote sensing research in hydrometeorology. Photogramm Eng Remote Sensing 69(6):613–646

Kustas WP, Hatfield JL, Prueger JH (2005) The Soil Moisture–Atmosphere Coupling Experiment (SMACEX): background, hydrometeorological conditions, and preliminary findings. J Hydrometeorol 6:825–839. doi:10.1175/JHM460.1

Lagouarde, J.P., Brunet, Y., 1991. A simple model for estimating the daily upward longwave surface radiations from NOAA–AVHRR data. International Journal of Remote Sensing 12, 1853–1864.

Lhomme JP, Monteny B, Amadou M (1994) Estimating sensible heat flux from radiometric temperature over sparse millet. Agric For Meteorol 44:197–216

Li, Z.L., Becker, F., 1993. Feasibility of land surface temperature and emissivity determination from AVHRR data. Remote Sensing of Environment 43, 67–85.

Li F, Kustas WP, Prueger JH, Neale CMU, Jackson TJ (2005) Utility of remote sensing based two-source energy balance model under low and high vegetation cover conditions. J Hydrometeorol 6(6):878–891. doi:10.1175/JHM464.1

Li Z.L., Tang R., Wan Z., Bi Y., Zhou C., Tang B., Yan G. and Zang X. (2009), A Review of Current Methodologies for Regional Evapotranspiration Estimation from Remotely Sensed Data, Sensors 2009, 9, 3801-3853; doi:10.3390/s90503801

McCabe MF, Wood EF (2006) Scale influences on the remote estimation of evapotranspiration using multiple satellite sensors. Remote Sens Environ 105(4):271–285. doi:10.1016/j.rse.2006.07.006

McVicar TR, Jupp DLB (1998) The current and potential operational uses of remote sensing to aid decisions on drought exceptional circumstances in Australia: a review. Agric Syst 57:399–468. doi:10.1016/S0308-521X(98)00026-2

Monteith JL (1965) Evaporation and the environment. In: Fogg GE (ed) The state and movement of water in living organisms, 19th symposium of the society for experimental biology. University Press, Cambridge, pp 205–234

Monteith, J.L., 1981. Evaporation and surface temperature. Quart. J. Roy. Meteorolog. Soc., 107, 1–27.

Norman JM, Kustas WP, Humes KS (1995) A two-source approach for estimating soil and vegetation energy fluxes from observations of directional radiometric surface temperature. Agric For Meteorol 77:263–293. doi:10.1016/0168-1923(95)02265-Y

Norman JM, Kustas WP, Prueger JH, Diak GR (2000) Surface flux estimation using radiometric temperature: a dual-temperature-difference method to minimize measurement errors. Water Resour Res 36:2263–2274. doi:10.1029/2000WR900033

Overgaard J, Rosbjerg D, Butts MB (2006) Land-surface modelling in hydrological perspective—a review. Biogeosciences 3:229–241

Penman HL (1948) Natural evaporation from open water, bare soil and grass. Proc R Soc Lond A Math Phys Sci 193:120–146. doi:10.1098/rspa.1948.0037

Roerink GJ, Su Z, Menenti M (2000) S-SEBI: a simple remote sensing algorithm to estimate the surface energy balance. Phys Chem Earth, Part B Hydrol Oceans Atmos 25(2):147–157. doi:10.1016/S1464-1909(99)00128-8

Seguin B, Baelz S, Monget JM, Petit V (1982a) Utilisation de la thermographie IR pour l'estimation de l'e´vaporation re´gionale I Mise au point me´thodologique sur le site de la Crau. Agronomie 2(1):7–16. doi:10.1051/agro:19820102

Serban C., Maftei C., Barbulescu A. (2010), Assessment of Evapotranspiration Using Remote Sensing Data and Grid Computing and Apglication, WSEAS Transactions on computers, ISSN: 1109-2750, Issue 11, Volume 9, November 2010, pg.1245-1254

Shuttleworth WJ, Wallace JS (1985) Evaporation from sparse crops-an energy combination theory. Q J R Meteorol Soc 111:839–855. doi:10.1256/smsqj.46909

Smith, R. C. G. & Choudhury, B. J. (1991) Analysis of normalized difference and surface temperature observations over southeastern Australia. Int. J. Remote Sens. 12, 2021-2044.

Sobrino JA, Gomez M, Jimenez-Munoz JC, Olioso A (2007) Application of a simple algorithm to estimate daily evapotranspiration from NOAA-AVHRR images for the Iberian Peninsula. Remote Sens Environ 110:139–148. doi:10.1016/j.rse.2007.02.017

Stancalie GH, Marica A, Toulios L, (2010) Using earth observation data and CROPWAT model to estimate the actual crop evapotranspiration. Physics and Chemistry of the Earth, 35:25-30, doi:10.1016/j.pce.2010.03.013.

Stewart JB, Kustas WP, Humes KS, Nichols WD, Moran MS, De Bruin HAR (1994) Sensible heat flux–radiometric surface temperature relationships for eight semi-arid areas. J Appl Meteorol 33:1110–1117. doi :10.1175/1520-0450(1994)033\1110:SHFRST [2.0.CO;2

Su Z (2002) The Surface Energy Balance System (SEBS) for estimation of turbulent heat fluxes. Hydrol Earth Syst Sci 6(1):85–99 (HESS)

Su H, McCabe MF, Wood EF, Su Z, Prueger JH (2005) Modeling evapotranspiration during SMACEX: comparing two approaches for local- and regional-scale prediction. J Hydrometeorol 6(6):910–922. doi:10.1175/JHM466.1

Su Z (2008) The Surface Energy Balance System (SEBS) for estimation of turbulent heat fluxes and evapotranspiration, Dragon 2, Advanced Trainig Course in Land Remote Sensing,
http://dragon2.esa.int/landtraining2008/pdf/D3L2b_SU_SEBS.pdf

Wang K, Li Z, Cribb M (2006) Estimation of evaporative fraction from a combination of day and night land surface temperature and NDVI: a new method to determine the Priestley–Taylor parameter. Remote Sens Environ 102:293–305. doi:10.1016/j.rse.2006.02.007

Wood, E.F., Hongbo, Su, McCabe, M., Su, B., 2003. Estimating evaporation from satellite remote sensing. In: Geoscience and Remote Sensing Symposium 2003. IGARSS Proceedings of the IEEE International, vol. 2, pp. 163–1165.

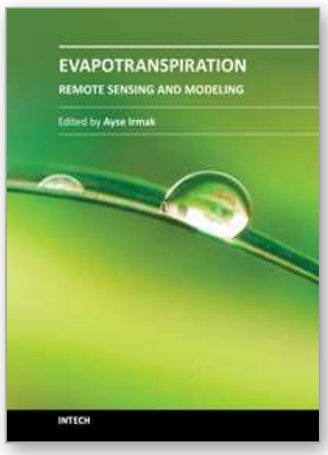

Evapotranspiration - Remote Sensing and Modeling

Edited by Dr. Ayse Irmak

ISBN 978-953-307-808-3
Hard cover, 514 pages
Publisher InTech
Published online 18, January, 2012
Published in print edition January, 2012

This edition of Evapotranspiration - Remote Sensing and Modeling contains 23 chapters related to the modeling and simulation of evapotranspiration (ET) and remote sensing-based energy balance determination of ET. These areas are at the forefront of technologies that quantify the highly spatial ET from the Earth's surface. The topics describe mechanics of ET simulation from partially vegetated surfaces and stomatal conductance behavior of natural and agricultural ecosystems. Estimation methods that use weather based methods, soil water balance, the Complementary Relationship, the Hargreaves and other temperature-radiation based methods, and Fuzzy-Probabilistic calculations are described. A critical review describes methods used in hydrological models. Applications describe ET patterns in alpine catchments, under water shortage, for irrigated systems, under climate change, and for grasslands and pastures. Remote sensing based approaches include Landsat and MODIS satellite-based energy balance, and the common process models SEBAL, METRIC and S-SEBS. Recommended guidelines for applying operational satellite-based energy balance models and for overcoming common challenges are made.

InTech Europe
University Campus STeP Ri
Slavka Krautzeka 83/A
51000 Rijeka, Croatia
Phone: +385 (51) 770 447
Fax: +385 (51) 686 166
www.intechopen.com

InTech China
Unit 405, Office Block, Hotel Equatorial Shanghai
No.65, Yan An Road (West), Shanghai, 200040, China
中国上海市延安西路65号上海国际贵都大饭店办公楼405单元
Phone: +86-21-62489820
Fax: +86-21-62489821

IntechOpen